

## Study of cosmic backreaction on the future evolution of an accelerating universe using multiple domains

Nilok Bose\* and A. S. Majumdar

*S. N. Bose National Centre for Basic Sciences,  
Block JD, Sector III, Salt Lake,  
Kolkata 700098, India*

*\*E-mail: nilok@bose.res.in*

We investigate the effect of backreaction due to inhomogeneities on the evolution of the present Universe by considering the Universe to be partitioned into multiple domains within the Buchert framework. Taking the observed present acceleration of the universe as an essential input, we study the effect of inhomogeneities on the future evolution. We find that the backreaction from inhomogeneities causes the acceleration to slow down in the future for a range of initial configurations and model parameters, and even lead in certain cases to the emergence of a future decelerating epoch. We consider two different partitioning of the Universe and perform a comparative analysis for the two cases on the behaviour of the acceleration and backreaction of the Universe.

PACS numbers: 98.80.-k, 95.36.+x, 98.80.Es

### 1. Introduction

By now the present acceleration of the Universe is quite well established observationally,<sup>1</sup> and the cause for it is attributed to a mysterious component called Dark Energy whose true nature is still unknown to us. A cosmological constant serves as the simplest possible explanation for the current acceleration but it is endowed with several conceptual problems.<sup>2</sup> There is no dearth of innovative ideas to explain the current acceleration<sup>3</sup> but our present state of knowledge offers no clear indication on the nature of the big rip that our Universe seems to be headed for.

We know from observations that the Universe is inhomogeneous up to the scales of super-clusters of galaxies, which suggests that some modification is needed for our standard cosmological framework that is based on the globally smooth Friedmann–Robertson–Walker (FRW) metric. Since the equations of general relativity are non-linear in nature therefore if we take the global average of the Einstein tensor then those results are very unlikely to be the same as that obtained by taking the average over all the different local metrics and then computing the global Einstein tensor. This realization has led to the investigation of the question of how backreaction originating from density inhomogeneities could modify the evolution of the universe as described by the background FRW metric at large scales.

Several approaches have been developed to facilitate the study of the effects of inhomogeneous matter distribution on the evolution of the Universe, such as Za-

2 *Nilok Bose, A. S. Majumdar*

laletdinov's fully covariant macroscopic gravity;<sup>5</sup> Buchert's approach of averaging the scalar parts of Einstein's equations,<sup>6,7</sup> the perturbation techniques proposed by Kolb et. al.,<sup>8</sup> and recently another procedure based on light-cone averaging has been proposed.<sup>19</sup> It has also been argued, by using the framework developed by Buchert, that backreaction from inhomogeneities could be responsible for the current acceleration of the Universe.<sup>9</sup> A different perspective of the Buchert framework developed by Wiltshire<sup>10</sup> also leads to an apparent acceleration due to the different lapse of time in underdense and overdense regions.

Since inhomogeneities lead to the formation of structures in the present era therefore the effects of backreaction will also gain strength in the present era, and hence if backreaction is indeed responsible for the current accelerated expansion then it will provide an interesting platform to study this issue, without invoking additional physics. While there is some debate on the impact of inhomogeneities on observables of an overall homogeneous FRW model,<sup>11–13</sup> and there are also similar questions with regard to the magnitude of backreaction modulated by the effect of shear between overdense and underdense regions,<sup>14</sup> recent studies<sup>6–10,13,15,16</sup> have provided a strong motivation for exploring further the role of inhomogeneities on the evolution of the present Universe. Nonetheless further investigations with the input of data from future observational probes are required for a conclusive picture to emerge.

Recently we studied the backreaction scenario within the Buchert framework using a simple two-scale model.<sup>17</sup> Our model indicated the possibility of a transition to a future decelerated era. The Buchert framework has been further extended in [16](#) so as to facilitate the study of backreaction in the case where the universe is considered to be divided into multiple domains and subdomains. But the model that was considered in [16](#) was a simple model consisting of one overdense subdomain and one underdense subdomain, like that used in [17](#). Such a simple model is attractive because it simplifies the evolution equations and eases the process of understanding the effect of backreaction on the evolution of the Universe. But the real Universe cannot be partitioned simply into one overdense subdomain and one underdense subdomain. To the best of our knowledge, so far there has been no study on the effect of backreaction from inhomogeneities by considering multiple subdomains. Using the formalism proposed in [16](#), in the present paper we improve upon our previous two-scale model and consider the Universe as a global domain  $\mathcal{D}$  which is partitioned into multiple overdense and underdense regions, and all these subdomains are taken to evolve differently to each other. This is done in order to recreate the real Universe as much as possible in our simple model. Our aim here is to study the future evolution of the Universe by taking into consideration its current accelerated expansion. The accelerated expansion of the Universe can be assumed to be caused by backreaction or any other mechanism.<sup>3</sup> We consider two different partitioning cases of the Universe and explore the future evolution of the Universe for these two cases and then perform a comparative analysis for the two.

The paper is organized as follows. In Section II we briefly recapitulate the essential details of the Buchert framework<sup>6,7,15</sup> including the evolution equations when the Universe is partitioned into multiple subdomains. Next, in Section III we follow the approach of <sup>16</sup> and investigate the future evolution of the Universe assuming its present stage of global acceleration. Subsequently, in Section IV we perform a quantitative comparison of various dynamical features of our model for the two partitioning cases that we consider. Finally, we summarize our results and make some concluding remarks in Section V.

## 2. The Backreaction Framework

### 2.1. Averaged Einstein equations

In the framework developed by Buchert<sup>6,7,15,16</sup> for the Universe filled with an irrotational fluid of dust, the space-time is foliated into flow-orthogonal hypersurfaces featuring the line-element

$$ds^2 = -dt^2 + g_{ij}dX^i dX^j \quad (1)$$

where the proper time  $t$  labels the hypersurfaces and  $X^i$  are Gaussian normal coordinates (locating free-falling fluid elements or generalized fundamental observers) in the hypersurfaces, and  $g^{ij}$  is the full inhomogeneous three metric of the hypersurfaces of constant proper time. The framework is applicable to perfect fluid matter models.

For a compact spatial domain  $\mathcal{D}$ , comoving with the fluid, there is one fundamental quantity characterizing it and that is its volume. This volume is given by

$$|\mathcal{D}|_g = \int_{\mathcal{D}} d\mu_g \quad (2)$$

where  $d\mu_g = \sqrt{{}^{(3)}g}(t, X^1, X^2, X^3)dX^1 dX^2 dX^3$ . From the domain's volume one may define a scale-factor

$$a_{\mathcal{D}}(t) = \left( \frac{|\mathcal{D}|_g}{|\mathcal{D}_i|_g} \right)^{1/3} \quad (3)$$

that encodes the average stretch of all directions of the domain.

Using the Einstein equations, with a pressure-less fluid source, we get the following equations<sup>6,15,16</sup>

$$3 \frac{\ddot{a}_{\mathcal{D}}}{a_{\mathcal{D}}} = -4\pi G \langle \rho \rangle_{\mathcal{D}} + \mathcal{Q}_{\mathcal{D}} + \Lambda \quad (4)$$

$$3H_{\mathcal{D}}^2 = 8\pi G \langle \rho \rangle_{\mathcal{D}} - \frac{1}{2} \langle \mathcal{R} \rangle_{\mathcal{D}} - \frac{1}{2} \mathcal{Q}_{\mathcal{D}} + \Lambda \quad (5)$$

$$0 = \partial_t \langle \rho \rangle_{\mathcal{D}} + 3H_{\mathcal{D}} \langle \rho \rangle_{\mathcal{D}} \quad (6)$$

Here the average of the scalar quantities on the domain  $\mathcal{D}$  is defined as,

$$\langle f \rangle_{\mathcal{D}}(t) = \frac{\int_{\mathcal{D}} f(t, X^1, X^2, X^3) d\mu_g}{\int_{\mathcal{D}} d\mu_g} = |\mathcal{D}|_g^{-1} \int_{\mathcal{D}} f d\mu_g \quad (7)$$

4 Nilok Bose, A. S. Majumdar

and where  $\rho$ ,  $\mathcal{R}$  and  $H_{\mathcal{D}}$  denote the local matter density, the Ricci-scalar of the three-metric  $g_{ij}$ , and the domain dependent Hubble rate  $H_{\mathcal{D}} = \dot{a}_{\mathcal{D}}/a_{\mathcal{D}}$  respectively. The kinematical backreaction  $\mathcal{Q}_{\mathcal{D}}$  is defined as

$$\mathcal{Q}_{\mathcal{D}} = \frac{2}{3} \left( \langle \theta^2 \rangle_{\mathcal{D}} - \langle \theta \rangle_{\mathcal{D}}^2 \right) - 2\sigma_{\mathcal{D}}^2 \quad (8)$$

where  $\theta$  is the local expansion rate and  $\sigma^2 = 1/2\sigma_{ij}\sigma^{ij}$  is the squared rate of shear. It should be noted that  $H_{\mathcal{D}}$  is defined as  $H_{\mathcal{D}} = 1/3 \langle \theta \rangle_{\mathcal{D}}$ .  $\mathcal{Q}_{\mathcal{D}}$  encodes the departure from homogeneity and for a homogeneous domain its value is zero.

One also has an integrability condition that is necessary to yield (5) from (4) and that relation reads as

$$\frac{1}{a_{\mathcal{D}}^6} \partial_t (a_{\mathcal{D}}^6 \mathcal{Q}_{\mathcal{D}}) + \frac{1}{a_{\mathcal{D}}^2} \partial_t (a_{\mathcal{D}}^2 \langle \mathcal{R} \rangle_{\mathcal{D}}) = 0 \quad (9)$$

From this equation we see that the evolution of the backreaction term, and hence extrinsic curvature inhomogeneities, is coupled to the average intrinsic curvature. Unlike the FRW evolution equations where the curvature term is restricted to an  $a_{\mathcal{D}}^{-2}$  behaviour, here it is more dynamical because it can be any function of  $a_{\mathcal{D}}$ .

## 2.2. Separation formulae for arbitrary partitions

The ‘‘global’’ domain  $\mathcal{D}$  is assumed to be separated into subregions  $\mathcal{F}_{\ell}$ , which themselves consist of elementary space entities  $\mathcal{F}_{\ell}^{(\alpha)}$  that may be associated with some averaging length scale. In mathematical terms  $\mathcal{D} = \cup_{\ell} \mathcal{F}_{\ell}$ , where  $\mathcal{F}_{\ell} = \cup_{\alpha} \mathcal{F}_{\ell}^{(\alpha)}$  and  $\mathcal{F}_{\ell}^{(\alpha)} \cap \mathcal{F}_m^{(\beta)} = \emptyset$  for all  $\alpha \neq \beta$  and  $\ell \neq m$ . The average of the scalar valued function  $f$  on the domain  $\mathcal{D}$  (7) may then be split into the averages of  $f$  on the subregions  $\mathcal{F}_{\ell}$  in the form,

$$\langle f \rangle_{\mathcal{D}} = \sum_{\ell} |\mathcal{D}|_g^{-1} \sum_{\alpha} \int_{\mathcal{F}_{\ell}^{(\alpha)}} f d\mu_g = \sum_{\ell} \lambda_{\ell} \langle f \rangle_{\mathcal{F}_{\ell}} \quad (10)$$

where  $\lambda_{\ell} = |\mathcal{F}_{\ell}|_g/|\mathcal{D}|_g$ , is the volume fraction of the subregion  $\mathcal{F}_{\ell}$ . The above equation directly provides the expression for the separation of the scalar quantities  $\rho$ ,  $\mathcal{R}$  and  $H_{\mathcal{D}} = 1/3 \langle \theta \rangle_{\mathcal{D}}$ . However,  $\mathcal{Q}_{\mathcal{D}}$ , as defined in (8), does not split in such a simple manner due to the  $\langle \theta \rangle_{\mathcal{D}}^2$  term. Instead the correct formula turns out to be

$$\mathcal{Q}_{\mathcal{D}} = \sum_{\mathcal{D}} \lambda_{\ell} \mathcal{Q}_{\ell} + 3 \sum_{\ell \neq m} \lambda_{\ell} \lambda_m (H_{\ell} - H_m)^2 \quad (11)$$

where  $\mathcal{Q}_{\ell}$  and  $H_{\ell}$  are defined in  $\mathcal{F}_{\ell}$  in the same way as  $\mathcal{Q}_{\mathcal{D}}$  and  $H_{\mathcal{D}}$  are defined in  $\mathcal{D}$ . The shear part  $\langle \sigma^2 \rangle_{\mathcal{F}_{\ell}}$  is completely absorbed in  $\mathcal{Q}_{\ell}$ , whereas the variance of the local expansion rates  $\langle \theta^2 \rangle_{\mathcal{D}} - \langle \theta \rangle_{\mathcal{D}}^2$  is partly contained in  $\mathcal{Q}_{\ell}$  but also generates the extra term  $3 \sum_{\ell \neq m} \lambda_{\ell} \lambda_m (H_{\ell} - H_m)^2$ . This is because the part of the variance that is present in  $\mathcal{Q}_{\ell}$ , namely  $\langle \theta^2 \rangle_{\mathcal{F}_{\ell}} - \langle \theta \rangle_{\mathcal{F}_{\ell}}^2$  only takes into account points inside  $\mathcal{F}_{\ell}$ . To restore the variance that comes from combining points of  $\mathcal{F}_{\ell}$  with others in  $\mathcal{F}_m$ , the extra term containing the averaged Hubble rate emerges. Note here that the

above formulation of the backreaction holds in the case when there is no interaction between the overdense and the underdense subregions.

Analogous to the scale-factor for the global domain, a scale-factor  $a_\ell$  for each of the subregions  $\mathcal{F}_\ell$  can be defined such that  $|\mathcal{D}|_g = \sum_\ell |\mathcal{F}_\ell|_g$ , and hence,

$$a_{\mathcal{D}}^3 = \sum_\ell \lambda_{\ell_i} a_\ell^3 \quad (12)$$

where  $\lambda_{\ell_i} = |\mathcal{F}_{\ell_i}|_g/|\mathcal{D}_i|_g$  is the initial volume fraction of the subregion  $\mathcal{F}_\ell$ . If we now twice differentiate this equation with respect to the foliation time and use the result for  $\dot{a}_\ell$  from (5), we then get the expression that relates the acceleration of the global domain to that of the sub-domains:

$$\frac{\ddot{a}_{\mathcal{D}}}{a_{\mathcal{D}}} = \sum_\ell \lambda_\ell \frac{\ddot{a}_\ell(t)}{a_\ell(t)} + \sum_{\ell \neq m} \lambda_\ell \lambda_m (H_\ell - H_m)^2 \quad (13)$$

### 3. Future evolution within the Buchert framework

We will now explore the future evolution of the Universe after the current stage of acceleration sets in. It is not necessary to assume that the acceleration is caused by backreaction.<sup>9,16</sup> For the purpose of our present analysis, it suffices to consider the observed accelerated phase of the universe<sup>4</sup> that could occur due to any of a variety of mechanisms.<sup>3</sup>

Following the Buchert framework<sup>6,16</sup> as discussed above, the global domain  $\mathcal{D}$  is divided into multiple domains. We consider  $\mathcal{D}$  to be partitioned into equal numbers of overdense and underdense domains. We label all overdense domains as  $\mathcal{M}$  (called ‘Wall’) and all underdense domains as  $\mathcal{E}$  (called ‘Void’), such that  $\mathcal{D} = (\cup_j \mathcal{M}^j) \cup (\cup_j \mathcal{E}^j)$ . In this case one obtains  $H_{\mathcal{D}} = \sum_j \lambda_{\mathcal{M}_j} H_{\mathcal{M}_j} + \sum_j \lambda_{\mathcal{E}_j} H_{\mathcal{E}_j}$ , with similar expressions for  $\langle \rho \rangle_{\mathcal{D}}$  and  $\langle \mathcal{R} \rangle_{\mathcal{D}}$  and also  $\sum_j \lambda_j = 1$ . For such a partitioning the global acceleration (13) can be written as

$$\begin{aligned} \frac{\ddot{a}_{\mathcal{D}}}{a_{\mathcal{D}}} &= \sum_j \lambda_{\mathcal{M}_j} \frac{\ddot{a}_{\mathcal{M}_j}}{a_{\mathcal{M}_j}} + \sum_j \lambda_{\mathcal{E}_j} \frac{\ddot{a}_{\mathcal{E}_j}}{a_{\mathcal{E}_j}} \\ &+ \sum_{j \neq k} \lambda_{\mathcal{M}_j} \lambda_{\mathcal{M}_k} (H_{\mathcal{M}_j} - H_{\mathcal{M}_k})^2 \\ &+ \sum_{j \neq k} \lambda_{\mathcal{E}_j} \lambda_{\mathcal{E}_k} (H_{\mathcal{E}_j} - H_{\mathcal{E}_k})^2 \\ &+ 2 \sum_{j, k} \lambda_{\mathcal{M}_j} \lambda_{\mathcal{E}_k} (H_{\mathcal{M}_j} - H_{\mathcal{E}_k})^2 \end{aligned} \quad (14)$$

We assume that the scale-factors of the regions  $\mathcal{E}^j$  and  $\mathcal{M}^j$  are, respectively, given by  $a_{\mathcal{E}_j} = c_{\mathcal{E}_j} t^{\alpha_j}$  and  $a_{\mathcal{M}_j} = c_{\mathcal{M}_j} t^{\beta_j}$  where  $\alpha_j$ ,  $\beta_j$ ,  $c_{\mathcal{E}_j}$  and  $c_{\mathcal{M}_j}$  are constants. The volume fraction of the subdomain  $\mathcal{M}^j$  is given by  $\lambda_{\mathcal{M}_j} = \frac{|\mathcal{M}^j|_g}{|\mathcal{D}|_g}$ , which can be rewritten in terms of the corresponding scale factors as  $\lambda_{\mathcal{M}_j} = \frac{a_{\mathcal{M}_j}^3 |\mathcal{M}_i^j|_g}{a_{\mathcal{D}}^3 |\mathcal{D}_i|_g}$ , and

6 Nilok Bose, A. S. Majumdar

similarly for the  $\mathcal{E}^j$  subdomains. We therefore find that the global acceleration equation (14) becomes

$$\begin{aligned} \frac{\ddot{a}_{\mathcal{D}}}{a_{\mathcal{D}}} = & \sum_j \frac{g_{\mathcal{M}_j}^3 t^{3\beta_j}}{a_{\mathcal{D}}^3} \frac{\beta_j(\beta_j - 1)}{t^2} + \sum_j \frac{g_{\mathcal{E}_j}^3 t^{3\alpha_j}}{a_{\mathcal{D}}^3} \frac{\alpha_j(\alpha_j - 1)}{t^2} \\ & + \sum_{j \neq k} \frac{g_{\mathcal{M}_j}^3 t^{3\beta_j}}{a_{\mathcal{D}}^3} \frac{g_{\mathcal{M}_k}^3 t^{3\beta_k}}{a_{\mathcal{D}}^3} \left( \frac{\beta_j}{t} - \frac{\beta_k}{t} \right)^2 \\ & + \sum_{j \neq k} \frac{g_{\mathcal{E}_j}^3 t^{3\alpha_j}}{a_{\mathcal{D}}^3} \frac{g_{\mathcal{E}_k}^3 t^{3\alpha_k}}{a_{\mathcal{D}}^3} \left( \frac{\alpha_j}{t} - \frac{\alpha_k}{t} \right)^2 \\ & + 2 \sum_{j, k} \frac{g_{\mathcal{M}_j}^3 t^{3\beta_j}}{a_{\mathcal{D}}^3} \frac{g_{\mathcal{E}_k}^3 t^{3\alpha_k}}{a_{\mathcal{D}}^3} \left( \frac{\beta_j}{t} - \frac{\alpha_k}{t} \right)^2 \end{aligned} \quad (15)$$

where  $g_{\mathcal{M}_j}^3 = \frac{\lambda_{\mathcal{M}_{j_0}} a_{\mathcal{D}_0}^3}{t_0^{3\beta_j}}$  and  $g_{\mathcal{E}_j}^3 = \frac{\lambda_{\mathcal{E}_{j_0}} a_{\mathcal{D}_0}^3}{t_0^{3\alpha_j}}$  are constants.

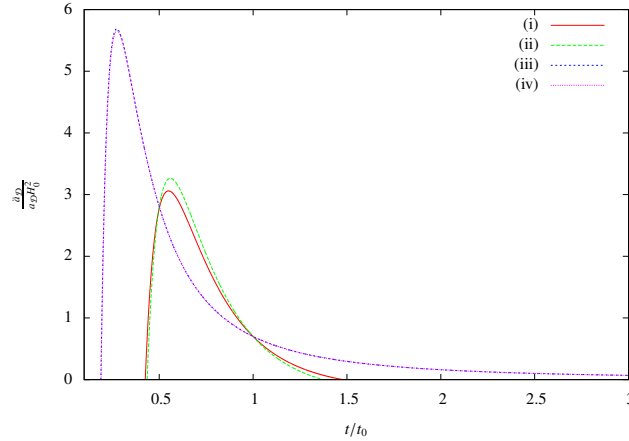


Fig. 1. The dimensionless global acceleration parameter  $\frac{\ddot{a}_{\mathcal{D}}}{a_{\mathcal{D}} H_0^2}$ , plotted vs. time (in units of  $t/t_0$  with  $t_0$  being the current age of the Universe). In curves (i) and (ii) the value of  $\alpha$  is in the range 0.990 - 0.999 and that of  $\beta$  is in the range 0.58 - 0.60. In curves (iii) and (iv) the value of  $\alpha$  is in the range 1.02 - 1.04 and that of  $\beta$  is in the range 0.58 - 0.60

We will perform a comparative study of two cases where (i) the global domain  $\mathcal{D}$  is considered to be divided into 50 overdense and underdense subdomains each and (ii) 100 overdense and underdense subdomains each. We will obtain numerical solutions of equation (15) for various ranges of parameter values. In order to do this we will consider the range of values for the parameters  $\alpha_j$  and  $\beta_j$  as a Gaussian distribution, which is of the form  $\frac{1}{\sigma\sqrt{2\pi}} \exp\left[-\frac{(x-\mu)^2}{2\sigma^2}\right]$ , where  $\sigma$  is the standard deviation and  $\mu$  is the mean (the range of values corresponds to the full width at half maximum of the distribution). We will also assign values for the volume fractions

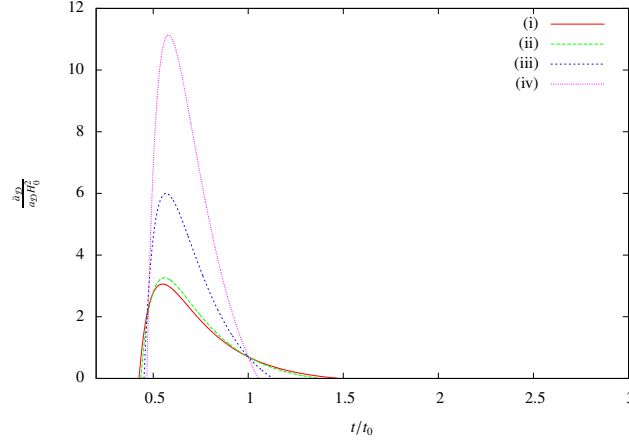


Fig. 2. Here also  $\frac{\ddot{a}_{\mathcal{D}}}{a_{\mathcal{D}} H_0^2}$  is plotted vs. time. In curves (i) and (ii) the value of  $\alpha$  lies in the range 0.990 - 0.999 and that of  $\beta$  is in the range 0.58 - 0.60. For curves (iii) and (iv) the value of  $\alpha$  is in the range 0.990 - 0.999 and that of  $\beta$  is in the range 0.55 - 0.65

$\lambda_{\mathcal{M}_j}$  and  $\lambda_{\mathcal{E}_j}$  based on a Gaussian distribution and impose the restriction that the total volume fraction of all the overdense subdomains at present time should be 0.09, a value that has been determined through numerical simulations in the earlier literature.<sup>16</sup> Note here that using our ansatz for the subdomain scale factors one may try to determine the global scale factor through Eq.(12). In order to do so, one needs to know the initial volume fractions  $\lambda_{\ell_i}$  which are in turn related to the  $c_{\mathcal{E}_j}$  and  $c_{\mathcal{M}_j}$ . However, in our approach based upon the Buchert framework<sup>6,7,16</sup> we do not need to determine  $c_{\mathcal{E}_j}$  and  $c_{\mathcal{M}_j}$ , but instead, obtain from Eq.(15) the global scale factor numerically by the method of recursive iteration, using as an ‘initial condition’ the observational constraint  $q_0 = -0.7$ , where  $q_0$  is the current value of the deceleration parameter. The expression for  $q_0$  is a completely analytic function of  $\alpha_j$ ,  $\beta_j$  and  $t_0$ , but since we are studying the effect of inhomogeneities therefore the Universe cannot strictly be described based on a FRW model and hence the current age of the Universe ( $t_0$ ) cannot be fixed based on current observations which use the FRW model to fix the age. Instead for each combination of values of the parameters  $\alpha_j$  and  $\beta_j$  we find out the value of  $t_0$  for our model from (15) by taking  $q_0 = -0.7$ .

It is of interest to study separately the behaviour of the backreaction term in the Buchert model.<sup>6,16</sup> The backreaction  $\mathcal{Q}_{\mathcal{D}}$  is obtained from (4) to be

$$\mathcal{Q}_{\mathcal{D}} = 3 \frac{\ddot{a}_{\mathcal{D}}}{a_{\mathcal{D}}} + 4\pi G \langle \rho \rangle_{\mathcal{D}} \quad (16)$$

Note that we are not considering the presence of any cosmological constant  $\Lambda$  as shown in (4). We can assume that  $\langle \rho \rangle_{\mathcal{D}}$  behaves like the matter energy density, i.e.  $\langle \rho \rangle_{\mathcal{D}} = \frac{c_{\rho}}{a_{\mathcal{D}}^3}$ , where  $c_{\rho}$  is a constant. Now, observations tell us that the current matter energy density fraction (baryonic and dark matter) is about 27% and that of dark energy is about 73%. Assuming the dark energy density to be of the order

8 Nilok Bose, A. S. Majumdar

of  $10^{-48} (GeV)^4$ , we get  $\rho_{\mathcal{D}_0} \simeq 3.699 \times 10^{-49} (GeV)^4$ . Thus, using the values for the global acceleration computed numerically, the future evolution of the backreaction term  $\mathcal{Q}_{\mathcal{D}}$  can also be computed (see Figs. 3 and 4, where we have plotted the backreaction density fraction  $\Omega_{\mathcal{Q}}^{\mathcal{D}} = -\frac{\mathcal{Q}_{\mathcal{D}}}{6H_{\mathcal{D}}^2}$ ).

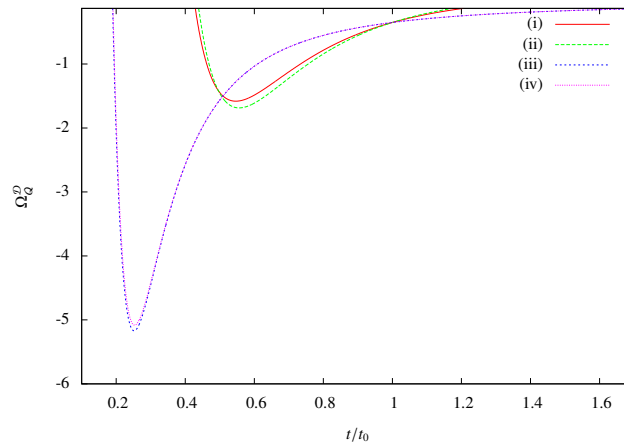


Fig. 3. Global backreaction density  $\Omega_{\mathcal{Q}}^{\mathcal{D}}$  plotted vs. time (in units of  $t/t_0$ ). In curves (i) and (ii) the value of  $\alpha$  is in the range 0.990 - 0.999 and that of  $\beta$  is in the range 0.58 - 0.60. In curves (iii) and (iv) the value of  $\alpha$  is in the range 1.02 - 1.04 and that of  $\beta$  is in the range 0.58 - 0.60

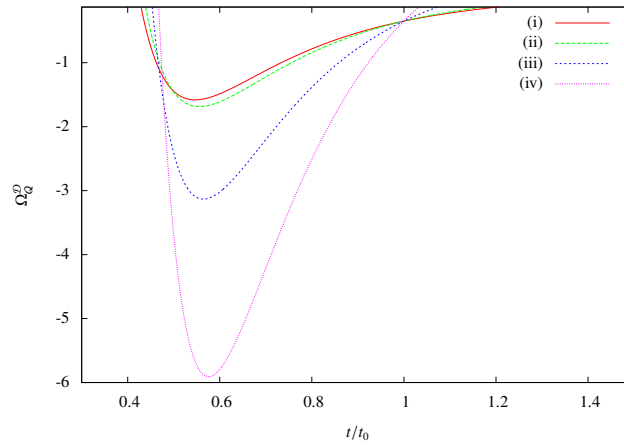


Fig. 4. Here also  $\Omega_{\mathcal{Q}}^{\mathcal{D}}$  is plotted vs. time. In curves (i) and (ii) the value of  $\alpha$  lies in the range 0.990 - 0.999 and that of  $\beta$  is in the range 0.58 - 0.60. For curves (iii) and (iv) the value of  $\alpha$  is in the range 0.990 - 0.999 and that of  $\beta$  is in the range 0.55 - 0.65



#### 4. Discussions

Let us now compare the nature of acceleration of the Universe for the two cases described in the previous section. The global acceleration for the two cases have been plotted in Figs. 1 and 2. In both the figures curves (i) and (iii) are for the case where  $\mathcal{D}$  is partitioned into 50 overdense and underdense subdomains each, and curves (ii) and (iv) correspond to the case where  $\mathcal{D}$  is partitioned into 100 overdense and underdense subdomains each. The values for the expansion parameters  $\beta_j$  of the overdense subdomains is taken to lie between 1/2 and 2/3 since the expansion is assumed to be faster than in the radiation dominated case, and is upper limited by the value for matter dominated expansion. In Fig. 1 the behaviour of global acceleration is shown for values of  $\alpha_j < 1$  and also  $\alpha_j > 1$ , keeping the range of values of  $\beta_j$  quite narrow and also the same for all four curves. We have kept the value of  $\alpha_j$  close to 1 when  $\alpha_j < 1$  because if  $\alpha_j$  is less than a certain value, which depends on the value of  $\beta_j$ , then the acceleration becomes undefined as we do not get real solutions from (15). In order to demonstrate this fact analytically let us consider a toy model where  $\mathcal{D}$  is divided into one overdense subdomain  $\mathcal{M}$  and one underdense subdomain  $\mathcal{E}$ . In this case (15) can be written as

$$\begin{aligned} \frac{\ddot{a}_{\mathcal{D}}}{a_{\mathcal{D}}} &= \frac{g_{\mathcal{M}}^3 t^{3\beta}}{a_{\mathcal{D}}^3} \frac{\beta(\beta-1)}{t^2} + \frac{g_{\mathcal{E}}^3 t^{3\alpha}}{a_{\mathcal{D}}^3} \frac{\alpha(\alpha-1)}{t^2} \\ &+ 2 \frac{g_{\mathcal{M}}^3 t^{3\beta}}{a_{\mathcal{D}}^3} \frac{g_{\mathcal{E}}^3 t^{3\alpha}}{a_{\mathcal{D}}^3} \left( \frac{\beta}{t} - \frac{\alpha}{t} \right)^2 \end{aligned} \quad (17)$$

Now we must have  $\lambda_{\mathcal{M}} + \lambda_{\mathcal{E}} = 1$ , so we can write  $\frac{g_{\mathcal{E}}^3 t^{3\beta}}{a_{\mathcal{D}}^3} = 1 - \frac{g_{\mathcal{M}}^3 t^{3\beta}}{a_{\mathcal{D}}^3}$ . Therefore the above equation now becomes

$$\begin{aligned} \frac{\ddot{a}_{\mathcal{D}}}{a_{\mathcal{D}}} &= \frac{g_{\mathcal{M}}^3 t^{3\beta}}{a_{\mathcal{D}}^3} \frac{\beta(\beta-1)}{t^2} + \left( 1 - \frac{g_{\mathcal{M}}^3 t^{3\beta}}{a_{\mathcal{D}}^3} \right) \frac{\alpha(\alpha-1)}{t^2} \\ &+ 2 \frac{g_{\mathcal{M}}^3 t^{3\beta}}{a_{\mathcal{D}}^3} \left( 1 - \frac{g_{\mathcal{M}}^3 t^{3\beta}}{a_{\mathcal{D}}^3} \right) \left( \frac{\beta}{t} - \frac{\alpha}{t} \right)^2 \end{aligned} \quad (18)$$

From this equation we see that the global acceleration vanishes at times given by

$$\begin{aligned} t^{3\beta} a_{\mathcal{D}}^3 &= \frac{1}{4(\beta-\alpha)g_{\mathcal{M}}^3} [(3\beta-\alpha-1) \\ &\pm \sqrt{(3\beta-\alpha-1)^2 + 8\alpha(\alpha-1)}] \end{aligned} \quad (19)$$

This shows us that we get real time solutions for  $\alpha \geq \frac{1}{3} \left[ (\beta+1) + 2\sqrt{2\beta(1-\beta)} \right]$ . If we now consider  $\beta = 0.5$  (its lowest possible

value) then we get  $\alpha \geq 0.971404521$  and if we consider  $\beta = 0.66$  (its highest possible value) then we get  $\alpha \geq 0.999950246$ . Hence as stated earlier, for a particular value of  $\beta$  we have a lower limit on the value of  $\alpha$ .

In Fig. 1, for  $\alpha_j < 1$  the acceleration becomes negative in the future for both cases of partitioning (curves (i) and (ii)). The acceleration reaches a greater value and at a slightly later time when  $\mathcal{D}$  is partitioned into 100 overdense and underdense subdomains (curve (ii)) and also becomes negative at an earlier time as compared to the case where  $\mathcal{D}$  is partitioned into 50 overdense and underdense subdomains (curve (i)). When  $\alpha_j > 1$  then we see that the acceleration curves for the two cases are almost identical, with the maximum value being very slightly larger for partition type (i) (curve (iii)). After reaching the maximum the acceleration decreases and goes asymptotically to a small positive value. When  $\alpha_j < 1$  then the first two terms of (15) are negative, but the last term, which is always positive, gains prominence as the number of subdomains increases thus increasing the acceleration. When  $\alpha_j > 1$  then only the first term in (15) is negative and hence the acceleration curves for the two partition cases (curves (iii) and (iv)) are very similar, the only visible difference being the slightly higher maximum value when  $\mathcal{D}$  is partitioned into a lower number of subdomains.

In Fig. 2 we have illustrated the behaviour of the global acceleration by taking narrow and broad ranges of values of  $\beta_j$  and keeping  $\alpha_j < 1$  and the same for all the curves. As seen in Fig. 1 here also the acceleration becomes negative in the future for all the curves because we have  $\alpha_j < 1$  for all of them, but we see that the difference between the acceleration curves for the two partition cases is very small when we consider a narrow range of values of  $\beta_j$  (curves (i) and (ii)) and the difference increases considerably when we consider a broad range of values of  $\beta_j$  (curve (iii) and (iv)). The acceleration attains a much greater value when  $\mathcal{D}$  is partitioned into a larger number of subdomains and also becomes negative quicker. The reason for the latter behaviour is that the broad range of values of  $\beta_j$  makes the third term in (15) gain more prominence when we consider a larger number of subdomains thus resulting in greater positive acceleration.

A similar comparison of the backreaction for the two models is presented in Figs. 3 and 4 where we have plotted the backreaction density for the duration over which the global acceleration is positive. We see in these figures that the backreaction density is negative and from the expression of  $\Omega_{\mathcal{D}}^{\mathcal{D}}$  and (8) it can be seen that the backreaction will be dominated by the variance of the local expansion rate  $\theta$ . In Fig. 3 we see that for  $\alpha_j < 1$ , the backreaction density reaches a minimum, which is also greater in magnitude, for partition type (ii) (curve (ii)) as compared to partition type (i) (curve (i)). For  $\alpha_j > 1$  the curves for the two cases are almost identical, the only difference being that for partition type (i) (curve (iii)) the backreaction density reaches a minimum of greater magnitude. In Fig. 4 we see that, just like the acceleration curves, the difference between the backreaction plots for the two partition cases is much smaller when we consider a narrow range of values of  $\beta_j$ ,

but the difference becomes quite large when we consider a broad range of values of  $\beta_j$ . The behaviour of the backreaction as illustrated in Figs. 3 and 4 is quite similar to the global acceleration, as seen in Figs. 1 and 2, and that is expected because from (16) we see that  $\mathcal{Q}_{\mathcal{D}}$  is linearly proportional to the global acceleration.

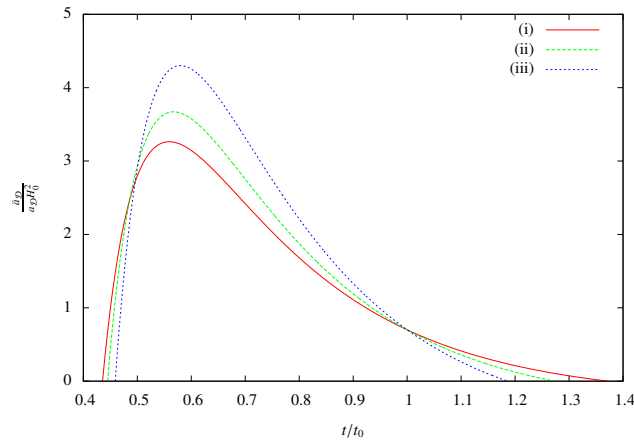


Fig. 5. We plot  $\frac{\ddot{a}_{\mathcal{D}}}{\ddot{a}_{\mathcal{D}} H_0^2}$  vs.  $t/t_0$  for various numbers of subdomains. In all the curves we have  $\alpha_j$  in the range 0.990 - 0.999, and  $\beta_j$  in the range 0.58 - 0.60. For curve (i) we consider 100 overdense and underdense subdomains, in (ii) 400 overdense and underdense subdomains and in (iii) 500 overdense and underdense subdomains each.

In order to see how the global acceleration behaves based on the number of subdomains we have in Fig. 5 plotted the global acceleration vs. time for three partition cases where we consider (i) 100 overdense and underdense subdomains, (ii) 400 overdense and underdense subdomains and (iii) 500 overdense and underdense subdomains each. For all three cases we have kept the range of values of  $\alpha_j$  and  $\beta_j$  the same and taken  $\alpha_j < 1$ . It is clearly seen from the plot that the global acceleration increases in magnitude as the number of subdomains increases, and the maximum is obtained later in time with increase in the number of subdomains. We also see that the acceleration becomes negative faster when the number of subdomains increases.

## 5. Conclusions

To summarize, in this work we have performed a detailed analysis of the various aspects of the future evolution of the presently accelerating universe in the presence of matter inhomogeneities. The effect of backreaction from inhomogeneities on the global evolution is calculated within the context of the Buchert framework by considering the universe to be divided into multiple underdense and overdense domains, each evolving independently, in order to recreate the real universe more accurately.<sup>6, 7, 15, 16</sup> We analyze the future evolution of the universe using the Buchert framework by computing the global acceleration and strength of backreaction. We

show that the Buchert framework allows for the possibility of the global acceleration vanishing at a finite future time, provided that none of the subdomains accelerate individually (both  $\alpha_j$  and  $\beta_j$  are less than 1).

Our analysis shows that if the  $\beta_j$  parameters as distributed over a narrow range of values and  $\alpha_j < 1$  then the global acceleration reaches a greater maximum, when the number of subdomains is larger, showing that the last term in (15), which is always positive, has more prominence for a large number of subdomains. This difference between the accelerations for the two partition cases decreases even more when  $\alpha_j > 1$ , because then only the first term in (15) has a negative contribution. However when we consider a broad range of values of  $\beta_j$  then the difference between the accelerations for the two cases becomes much larger, the acceleration being greater for a larger number of subdomains. The cause for this is attributed to the dominance of the third term in (15) when we have a larger number of subdomains and a broad range of values of  $\beta_j$ . We also saw that the behaviour of the backreaction mimics the behaviour of the global acceleration, and that is expected because as seen from (16), we have  $\mathcal{Q}_{\mathcal{D}}$  linearly proportional to the acceleration.

Our results indicate that backreaction can not only be responsible for the current accelerated expansion, as shown in earlier works,<sup>9,16</sup> but can also cause the acceleration to slow down and even lead to a future decelerated era in some cases. In drawing this conclusion it was not necessary for us to assume that the current acceleration is caused by backreaction, and the acceleration could have been caused by any other mechanism.<sup>3</sup>

## References

1. S. Perlmutter, et. al., *Nature* **391**, 51 (1998); A. G. Riess et. al., *Ap. J.* **116**, 1009 (1998); M. Hicken et al., *ApJ*, **700**, 1097 (2009); M. Seikel, D. J. Schwarz, *JCAP* **02**, 024 (2009).
2. S. Weinberg, *Rev. Mod. Phys.*, **61**, 1 (1989); T. Padmanabhan, *Adv. Sci. Lett.* **2**, 174 (2009).
3. V. Sahni, in Papantonopoulos E., ed., *Lecture Notes in Physics Vol. 653, The Physics of the Early Universe*. Springer, Berlin, p. 141 (2004); E. J. Copeland, M. Sami, and S. Tsujikawa, *Int. J. Mod. Phys. D* **15**, 1753 (2006).
4. M. Seikel, D. J. Schwarz, *J. Cosmol. Astropart. Phys.*, 02, 024 (2009)
5. R. Zalaletdinov, *Gen. Rel. Grav.*, **24**, 1015 (1992); *Gen. Rel. Grav.*, **25**, 673 (1993).
6. T. Buchert, *Gen. Rel. Grav.*, **32**, 105 (2000); T. Buchert, *Gen. Rel. Grav.* **33**, 1381. (2001).
7. T. Buchert, M. Carfora, *Phys. Rev. Lett.* **90**, 031101 (2003).
8. E. W. Kolb, S. Matarrese, A. Notari and A. Riotto, *Phys. Rev. D* **71**, 023524 (2005).
9. S. Rasanen, *J. Cosmol. Astropart. Phys.*, **0402**, 003 (2004); S. Rasanen, *J. Cosmol. Astropart. Phys.*, **0804**, 026 (2008); S. Rasanen, *J. Cosmol. Astropart. Phys.*, **02**, 011 (2009); S. Rasanen, *Phys. Rev. D* **81**, 103512 (2010).
10. D. L. Wiltshire, *New J. Phys.* **9**, 377 (2007); D. L. Wiltshire, *Phys. Rev. Lett.* **99**, 251101 (2007).
11. A. Ishibashi, R. M. Wald, *Classical Quantum Gravity*, **23**, 235 (2006).
12. A. Paranjape, T. P. Singh, *Phys. Rev. D* **78**, 063522 (2008); T. P. Singh, arXiv:1105.3450.

13. E. W. Kolb, S. Marra, S. Matarrese, Phys. Rev. D, **78**, 103002 (2008).
14. M. Mattsson, T. Mattsson, J. Cosmol. Astropart. Phys. **10**, 021 (2010).
15. T. Buchert, M. Carfora, Class. Quant. Grav. **25**, 195001 (2008).
16. A. Wiegand, T. Buchert, Phys. Rev. D **82**, 023523 (2010).
17. N. Bose, A. S. Majumdar, MNRAS Letters **418**, L45 (2011).
18. K. Bolejko, L. Andersson, J. Cosmol. Astropart. Phys. **10**, 003 (2008).
19. M. Gasperini et al., J. Cosmol. Astropart. Phys. **07**, 008 (2011).